arXiv:cond-mat/0309684v1 [cond-mat.str-el] 29 Sep 2003

Magnons in CMR pyrochlore $Tl_2Mn_2O_7$

C. I. Ventura
Centro Atómico Bariloche, 8400 - Bariloche, Argentina

M. Acquarone
IMEM-CNR, INFM - Unitá di Parma, Dipartimento di Fisica, Università di Parma, Italy.

Well defined spin waves were observed when the spin dynamics of $Tl_2Mn_2O_7$, the first pyrochlore compound found to exhibit colossal magnetoresistance, was measured [J.W.Lynn et al., Phys. Rev. Lett. **80**,4582(1998)], in stark contrast with the experimental results on the larger family of magnetoresistive manganites with perovskite structure. In this work, we present our calculation for the spin waves in $Tl_2Mn_2O_7$, which we described using the microscopic generic model proposed recently for this compound [C.I.Ventura and M.A.Gusmao, Phys. Rev. B **65**, 14422(2002)]. We have employed a canonical transformation to determine perturbatively the effective spin-wave Hamiltonian, obtaining therefrom the renormalization of the ferromagnetic spin waves related to the localized Mn^{4+} spins, due to their coupling with the conduction electrons present. We have calculated the magnon dispersion relations along different paths in the first Brillouin zone, comparing them with those which are obtained for an ideal isotropic ferromagnet. This comparison evidences an agreement between the ferromagnetic magnons obtained from the generic model and the bare spin waves, such as had been found in neutron scattering experiments.

75.47.-m,75.50.-y,75.30.-m

I. INTRODUCTION

During the eight years passed since the first discovery of colossal magnetoresistance (CMR) in a manganite compound with pyrochlore crystal structure, $Tl_2Mn_2O_7$,[1–3] increasing evidence has been found of the many differences in physical properties with respect to the much better known family of CMR Mn-perovskites.[4] Starting from the different crystal structures, which in the pyrochlore case includes a tetrahedral (instead of cubic) array of the MnO_6 octahedra, with the possibility of the presence of magnetic frustration effects. Also the larger bend in the Mn-O-Mn bond angle (133 vs 170 degrees in perovskites) would tend to reduce the magnitude of any antiferromagnetic (AF) superexchange coupling.[3] The lack of Jahn-Teller distortions in the pyrochlores rules out the presence of Mn^{3+},[1,3,5] and therefore of the double-exchange mechanism proposed in connection with the perovskite Mn oxides. Another difference lies in the small spin-lattice correlation found in pyrochlores, where no abrupt changes in the lattice parameters appear near the critical temperature (Tc$\sim 125K$,[1–3]) being the MnO_6 octahedra almost temperature-independent while only varying smoothly their tilting angles inside the structure.[1] A large difference has been found early on, regarding the numbers of carriers: while CMR in perovskites is found to be optimal for about 30 percent doping, Hall experiments in $Tl_2Mn_2O_7$[3,6] indicated only about 10^{-3} to 10^{-5} conduction electrons per formula unit (with a one third reduction above Tc). No anomalous Hall contribution is present in the pyrochlores. We can also mention the opposite behaviour of Tc upon the application of pressure:[7,8] decreasing in the pyrochlores (even with a reversal of tendency at high pressures).

The large amount of experimental evidence gathered, including also studies of compounds where the different components of $Tl_2Mn_2O_7$ have been doped by substitution,[2,9–14] put into serious question if a common underlying mechanism for CMR could be present for perovskites and the pyrochlores, where transport and magnetism seem to be primarily related to different electronic orbitals,[3,10] coupled by hybridization. A series of theoretical proposals have been put forward and explored in connection with these results in pyrochlores.[15–18] In particular, the first microscopic model studied for $Tl_2Mn_2O_7$ was an intermediate valence model (IVM)[15] based on the suggestion[3] of the possibility of the presence of a small (x$\sim$0.01, related to the small number of carriers) amount of internal doping of the type $Tl^{3+}_{2-x}Tl^{2+}_{x}Mn^{4+}_{2-x}Mn^{5+}_{x}O_7$. The IVM[15] proved useful for the description of the main magnetotransport measured characteristics and the initially puzzling Hall data. This was done through the temperature- and magnetic field-dependent changes of the electronic structure, which in the ferromagnetic phase exhibited common features with the available band structure calculations,[19,20] including hybridization gaps in all bands except for the minority-spin carrier band. In the paramagnetic phase, all bands had developed spin-independent gaps and the reduction in the number of effective carriers could be explained placing the Fermi level slightly above the hybridization gap.[15] Later, the generic model for $Tl_2Mn_2O_7$[18] was put forward to explore a whole set of other proposals suggested for this compound.[1,3,7,16,21,17] This model includes a band of itinerant carriers hybridized with other strongly correlated

electronic orbitals. These appear forming a lattice of Mn^{4+} local magnetic moments, as well as occupying a narrow band, coupled through a strong Hund interaction.[18] A superexchange interaction between the Mn^{4+} spins is also included. The electronic structure was shown to share the main features of that obtained previously with the IVM model,[15] when using appropriate sets of parameters.[18]

In the present work, we address the problem of the study of the spin excitations in $Tl_2Mn_2O_7$, which were also found to be in stark contrast to those observed in perovskite manganites when measured in neutron scattering experiments.[22] The excitations observed in $Tl_2Mn_2O_7$ are magnons characteristic of a soft three-dimensional isotropic ferromagnet, softening at higher temperatures and appearing to collapse as the critical temperature is approached, being the ferromagnetic transition driven by thermal population of conventional spin waves. Here, we have calculated the spin wave dispersion relations for $Tl_2Mn_2O_7$ along different trajectories in the first Brillouin zone (BZ), using the generic model[18] with parameters found useful before for the description of the compound, and assuming a ferromagnetic superexchange interaction to be present. In Section II an outline is given of the method we have used to calculate the magnons: basically, we employed a canonical transformation to determine perturbatively the renormalization of the ferromagnetic spin waves related to the Mn^{4+} local moments, by their Hund coupling with the conduction electrons. In Section III, the general analytical expressions obtained in the previous section are evaluated for the specific case of $Tl_2Mn_2O_7$. A complete presentation and discussion of our results is included. A comparison of the renormalized spin waves calculated with the bare magnons, characteristic of a three-dimensional isotropic ferromagnet and alike to those measured in the available neutron scattering experiments,[22] evidences a good agreement. In Section IV a summary of our study and its conclusions are included, together with suggestions for new experiments which could test some of our predictions for other yet unexplored cases.

II. EFFECTIVE SPIN-WAVE HAMILTONIAN FOR $Tl_2Mn_2O_7$

We will begin by outlining our general scheme of calculation. The Hamiltonian as usual is split into non-interacting (H_0) and interacting (V) terms:

$$H \;=\; H_0 \,+\, V \tag{1}$$

Next we apply a unitary transformation yielding:

$$\tilde{H} \;=\; e^{iS} H e^{-iS}\,, \qquad S = S^{\dagger} \tag{2}$$

Developing $\tilde{H}$ to second order of perturbations we arrive at the following effective Hamiltonian:

$$\tilde{H} \;\sim\; \tilde{H}^{(2)} \;=\; H_0 \;+\; \frac{i}{2}\,[S,V] \;+\; 0(\,S^3\,)\;, \tag{3}$$

where S obeys: $V \,+\, i\,[S,H_0] \;=\; O$. Integrating this constraint in the interaction representation ($\mathcal{O}_{\mathcal{I}}(t) \;\equiv\; e^{iH_0 t}\mathcal{O}e^{-iH_0 t}$), yields:

$$S \;\sim\; S_I(t=0) \;=\; \frac{1}{\hbar}\,\int_{-\infty}^{0} dt\; V_I(t)\;. \tag{4}$$

For the present problem, we consider the generic model recently proposed[18] to describe $Tl_2Mn_2O_7$, which includes Hund and superexchange couplings as well as hybridization effects. Two kinds of electronic orbitals are present, as widely believed to be the case: one, directly related to the magnetism of the compound, involving localized Mn^{4+} moments and a narrow band strongly Hund-coupled to them.[18] The other, corresponding to more extended electronic orbitals, is related to the carriers which hybridize with the narrow band. A superexchange coupling between the localized spins is also present. The Hamiltonian[18] reads:

$$H \;=\; H_c \,+\, H_d \,+\, H_{cd} \,+\, H_S\,, \tag{5}$$

where:

$$H_c = -t_c \sum_{\langle i,j\rangle\sigma} (\; c^{\dagger}_{i\sigma} c_{j\sigma} \;+\; \text{H.c.}\;) - \;\mu \sum_{i\sigma} c^{\dagger}_{i\sigma} c_{i\sigma}\;,$$

$$H_d = -t_d \sum_{\langle i,j\rangle\sigma} (d^{\dagger}_{i\sigma} d_{j\sigma} + \text{H.c.}) + (\epsilon_d - \mu) \sum_{i\sigma} d^{\dagger}_{i\sigma} d_{i\sigma}\;,$$

$$H_{cd} = t_{cd} \sum_{i\sigma} \left(c^\dagger_{i\sigma} d_{i\sigma} + d^\dagger_{i\sigma} c_{i\sigma} \right) ,$$
$$H_S = -J_{\rm H} \sum_i \mathbf{S}_i \cdot \mathbf{s}^{(d)}_i - J_S \sum_{\langle i,j \rangle} \mathbf{S}_i \cdot \mathbf{S}_j \, . \tag{6}$$

Here H_c describes the band associated[18] to the weakly correlated carriers present in $Tl_2Mn_2O_7$, characterized by a hopping parameter t_c between nearest neighbors, and creation operators $c^\dagger_{i\sigma}$ for electrons with spin σ in the respective Wannier orbital centered on site i. H_d describes the narrow band associated to the strongly correlated orbitals,[18] with hopping $t_d (< t_c)$, and creation operators $d^\dagger_{i\sigma}$ for electrons with spin σ in the Wannier orbital of energy ϵ_d (with respect to the center of the c band,$\epsilon_c = 0$) localized on site i. The chemical potential of the system is denoted by μ, and is determined by the total electronic filling n. The hybridization H_{cd} between c and d electron bands is assumed to be local. H_S denotes the spin Hamiltonian, which includes the Hund (or Kondo-like) coupling, measured by J_H, between a local magnetic moment $\mathbf{S}_i$, of magnitude $M = 3/2$ associated to a Mn^{4+} ion at site i, and the itinerant spin $s = 1/2$ denoted by $\mathbf{s}^{(d)}_i$, corresponding to the d electron orbitals related to Mn (hybridized with O) in $Tl_2Mn_2O_7$.[18] A Heisenberg exchange term is also included in the spin Hamiltonian to allow for the superexchange coupling, measured by J_S, effective between the local moments of nearest neighbor Mn^{4+} ions.

Given this Hamiltonian (5) we identify H_0 as follows:

$$\begin{aligned} H_0 &= H^e_0 + H^b_0 \\ H^e_0 &= \sum_{q,\sigma} \left\{ \epsilon_c(q)\, c^\dagger_{q\sigma} c_{q\sigma} + [\epsilon_d(q) - \frac{\sigma J_H M}{2}]\, d^\dagger_{q\sigma} d_{q\sigma} + t_{cd}\, (c^\dagger_{q\sigma} d_{q\sigma} + d^\dagger_{q\sigma} c_{q\sigma}) \right\} \\ &\equiv \sum_{q,\sigma} [\, E^\alpha_{q\sigma}\, \alpha^\dagger_{q\sigma} \alpha_{q\sigma} + E^\beta_{q\sigma}\, \beta^\dagger_{q\sigma} \beta_{q\sigma} \,] \end{aligned} \tag{7}$$

where the bare tight binding energies read $\epsilon_\gamma(q) = \epsilon_\gamma - t_\gamma \sum_{n=1}^z e^{-i\mathbf{q}\cdot\mathbf{a}_n}$ (with $\gamma = c, d$, and $\mathbf{a}_n$ denoting the vectors connecting a site with its z nearest neighbors), while we have introduced the electronic eigenbands:

$$\begin{aligned} E^{\alpha}_{q\sigma} &= \frac{\epsilon_c(q) + \tilde{\epsilon}^\sigma_d(q) \mp \sqrt{(\epsilon_c(q) - \tilde{\epsilon}^\sigma_d(q))^2 + 4t^2_{cd}}}{2} , \\ \tilde{\epsilon}^\sigma_d(q) &= [\epsilon_d(q) - \frac{\sigma J_H M}{2}] , \end{aligned} \tag{8}$$

$$\begin{pmatrix} d^\dagger_{q\sigma} \\ c^\dagger_{q\sigma} \end{pmatrix} = \begin{pmatrix} \cos\eta_{q\sigma} & \sin\eta_{q\sigma} \\ -\sin\eta_{q\sigma} & \cos\eta_{q\sigma} \end{pmatrix} \begin{pmatrix} \alpha^\dagger_{q\sigma} \\ \beta^\dagger_{q\sigma} \end{pmatrix} , \tag{9}$$

with:

$$\tan(2\eta_{q\sigma}) = \frac{2t_{cd}}{\epsilon_c(q) - \tilde{\epsilon}^\sigma_d(q)} .$$

We have assumed a ferromagnetic superexchange interaction, consistently with the experimental neutron scattering data[22] indicating spin excitations characteristic of an isotropic ferromagnet. Using the Holstein-Primakoff transformation the local moments are expressed in term of bosonic ferromagnetic magnon operators as: $\mathbf{S}_l = \left(S^+_l, S^-_l, S^z_l\right) = \left(\sqrt{2M} b_l, \sqrt{2M} b^\dagger_l, M - b^\dagger_l b_l\right)$, at low temperatures. The superexchange term in H_S is then rewritten as:

$$H^b_0 = -\frac{J_S M^2 z N}{2} + \sum_q \omega_q\, b^\dagger_q\, b_q \, , \tag{10}$$

where ω_q is the bare ferromagnetic magnon energy on a lattice of N sites.

On the other hand, V is then identified as the Hund term of the Hamiltonian, that is:

$$V = -J_H \sum_l \left[s^z_l S^z_l + \frac{1}{2} \left(s^+_l S^-_l + s^-_l S^+_l \right) \right] \equiv V_z + V_{xy} \, , \tag{11}$$

where the longitudinal (V_z) and transversal (V_{xy}) terms respectively are:

$$V_z \;=\; -\frac{J_H M}{2}\,\sum_k\,\left(n^d_{k\uparrow}-n^d_{k\downarrow}\right)\;+\;\frac{J_H}{2N}\,\sum_{kpq,\sigma}\;\sigma\;\,d^\dagger_{k\sigma}d_{p+q\sigma}b^\dagger_q b_{k-p}\,, \tag{12}$$

$$V_{xy} \;=\; -J_H\,\sqrt{\frac{M}{2N}}\,\sum_{kq}\,\left(d^\dagger_{k\uparrow}d_{k+q\downarrow}b^\dagger_q+d^\dagger_{k\downarrow}d_{k+q\uparrow}b_{-q}\right)\,. \tag{13}$$

Here we employ the usual notation for Fermi number operators: $n^\gamma_{k\sigma}\,=\,\gamma^\dagger_{k,\sigma}\gamma_{k,\sigma}$, in this case with $\gamma = d$.

To avoid divergences in Eq. (4), we have redefined H^e_0 by incorporating the first term of V_z as a correction to the $d-$band energies, and continued working with the following effective interaction:

$$V' \;=\; V'_z + V_{xy}\,, \tag{14}$$

$$V'_z \;=\; \frac{J_H}{2N}\,\sum_{kpq,\sigma}\;\sigma\;\,d^\dagger_{k\sigma}d_{p+q\sigma}b^\dagger_q b_{k-p}\,. \tag{15}$$

By using V' in Eq. (4), we obtain:

$$S \;=\; S'_z\;+\;S_{xy}\,, \tag{16}$$

$$\begin{aligned} S'_z \;=\; -\frac{iJ_H}{2N}\,\sum_{k,p,q,\sigma}\,\sigma\Bigg[&\frac{\alpha^\dagger_{k\sigma}\alpha_{p+q\sigma}\,\cos\eta_{k\sigma}\cos\eta_{p+q\sigma}}{E^\alpha_{k\sigma}-E^\alpha_{p+q\sigma}+\omega_q-\omega_{k-p}}\;+\;\frac{\beta^\dagger_{k\sigma}\beta_{p+q\sigma}\,\sin\eta_{k\sigma}\sin\eta_{p+q\sigma}}{E^\beta_{k\sigma}-E^\beta_{p+q\sigma}+\omega_q-\omega_{k-p}} \\ +\;&\frac{\alpha^\dagger_{k\sigma}\beta_{p+q\sigma}\,\cos\eta_{k\sigma}\sin\eta_{p+q\sigma}}{E^\alpha_{k\sigma}-E^\beta_{p+q\sigma}+\omega_q-\omega_{k-p}}\;+\;\frac{\beta^\dagger_{k\sigma}\alpha_{p+q\sigma}\,\sin\eta_{k\sigma}\cos\eta_{p+q\sigma}}{E^\beta_{k\sigma}-E^\alpha_{p+q\sigma}+\omega_q-\omega_{k-p}}\Bigg]\,b^\dagger_q b_{k-p}\,, \end{aligned} \tag{17}$$

$$\begin{aligned} S_{xy} \;=\; -\frac{J_H\sqrt{M}}{i\sqrt{2N}}\,\sum_{k,q}\Bigg[&\frac{\alpha^\dagger_{k\uparrow}\alpha_{k+q\downarrow}\,\cos\eta_{k\uparrow}\cos\eta_{k+q\downarrow}}{E^\alpha_{k\uparrow}-E^\alpha_{k+q\downarrow}+\omega_q}\;+\;\frac{\beta^\dagger_{k\uparrow}\beta_{k+q\downarrow}\,\sin\eta_{k\uparrow}\sin\eta_{k+q\downarrow}}{E^\beta_{k\uparrow}-E^\beta_{k+q\downarrow}+\omega_q} \\ +\;&\frac{\alpha^\dagger_{k\uparrow}\beta_{k+q\downarrow}\,\cos\eta_{k\uparrow}\sin\eta_{k+q\downarrow}}{E^\alpha_{k\uparrow}-E^\beta_{k+q\downarrow}+\omega_q}\;+\;\frac{\beta^\dagger_{k\uparrow}\alpha_{k+q\downarrow}\,\sin\eta_{k\uparrow}\cos\eta_{k+q\downarrow}}{E^\beta_{k\uparrow}-E^\alpha_{k+q\downarrow}+\omega_q}\Bigg]\,b^\dagger_q \\ +\;\Bigg[&\frac{\alpha^\dagger_{k\downarrow}\alpha_{k+q\uparrow}\,\cos\eta_{k\downarrow}\cos\eta_{k+q\uparrow}}{E^\alpha_{k\downarrow}-E^\alpha_{k+q\uparrow}-\omega_{-q}}\;+\;\frac{\beta^\dagger_{k\downarrow}\beta_{k+q\uparrow}\,\sin\eta_{k\downarrow}\sin\eta_{k+q\uparrow}}{E^\beta_{k\downarrow}-E^\beta_{k+q\uparrow}-\omega_{-q}} \\ +\;&\frac{\alpha^\dagger_{k\downarrow}\beta_{k+q\uparrow}\,\cos\eta_{k\downarrow}\sin\eta_{k+q\uparrow}}{E^\alpha_{k\downarrow}-E^\beta_{k+q\uparrow}-\omega_{-q}}\;+\;\frac{\beta^\dagger_{k\downarrow}\alpha_{k+q\uparrow}\,\sin\eta_{k\downarrow}\cos\eta_{k+q\uparrow}}{E^\beta_{k\downarrow}-E^\alpha_{k+q\uparrow}-\omega_{-q}}\Bigg]\,b_{-q} \end{aligned} \tag{18}$$

Using Eq. (3), through a rather lengthy calculation we have obtained the following second order effective spin-wave Hamiltonian, after projection onto the fermion ground state $\mid \Psi_F\rangle$:

$$\tilde{H}^{(2)}_{sw} \;\equiv\; \langle\Psi_F\mid\tilde{H}^{(2)}\mid\Psi_F\rangle \;=\; const.\;+\;\sum_q\,\tilde{\omega}_q\,b^\dagger_q b_q\,. \tag{19}$$

It is interesting to notice that this Hamiltonian is directly diagonal in the original bare magnon operators, due to the fact that the projection onto states with fixed numbers of $\alpha_{k\sigma}$ and $\beta_{k\sigma}$-electrons turns out to eliminate any non-diagonal contributions. The renormalization of the magnon energies, originating from the coupling of the local Mn^{4+} moments with the itinerant electrons, has contributions due to both the longitudinal and the transverse parts of the Hund coupling term. Specifically, we have obtained the following "dressed" spin wave energies:

$$\tilde{\omega}_q \;=\; \omega_q\;+\;\frac{J^2_H M}{2N}\;t(q)\;+\;\left(\frac{J_H}{2N}\right)^2\,l(q)\,, \tag{20}$$

where the transverse renormalization factor $t(q)$ could be viewed as describing virtual one-electron scattering processes with the creation or absorption of one magnon, depending on the detailed filling of the different bare electron spin subbands, and reads:

$$t(q) = \sum_k \left[\frac{(n^\alpha_{k\uparrow} - n^\alpha_{k+q\downarrow}) \cos^2\eta_{k\uparrow} \cos^2\eta_{k+q\downarrow}}{E^\alpha_{k\uparrow} - E^\alpha_{k+q\downarrow} + \omega_q} + \frac{(n^\beta_{k\uparrow} - n^\beta_{k+q\downarrow}) \sin^2\eta_{k\uparrow} \sin^2\eta_{k+q\downarrow}}{E^\beta_{k\uparrow} - E^\beta_{k+q\downarrow} + \omega_q} \right.$$
$$\left. + \frac{(n^\alpha_{k\uparrow} - n^\beta_{k+q\downarrow}) \cos^2\eta_{k\uparrow} \sin^2\eta_{k+q\downarrow}}{E^\alpha_{k\uparrow} - E^\beta_{k+q\downarrow} + \omega_q} + \frac{(n^\beta_{k\uparrow} - n^\alpha_{k+q\downarrow}) \sin^2\eta_{k\uparrow} \cos^2\eta_{k+q\downarrow}}{E^\beta_{k\uparrow} - E^\alpha_{k+q\downarrow} + \omega_q} \right]. \quad (21)$$

The longitudinal magnon renormalization factor $l(q)$, on the other hand, involves virtual one electron-one magnon scattering processes, also depending on the detailed electron band fillings, and is given by:

$$l(q) = \sum_{k,p,\sigma} \sigma \left[\frac{n^\alpha_{k\sigma}(1 - n^\alpha_{p+q\sigma}) \cos^2\eta_{k\sigma} \cos^2\eta_{p+q\sigma}}{E^\alpha_{k\sigma} - E^\alpha_{p+q\sigma} + \omega_q - \omega_{k-p}} + \frac{n^\beta_{k\sigma}(1 - n^\beta_{p+q\sigma}) \sin^2\eta_{k\sigma} \sin^2\eta_{p+q\sigma}}{E^\beta_{k\sigma} - E^\beta_{p+q\sigma} + \omega_q - \omega_{k-p}} \right.$$
$$\left. + \frac{n^\alpha_{k\sigma}(1 - n^\beta_{p+q\sigma}) \cos^2\eta_{k\sigma} \sin^2\eta_{p+q\sigma}}{E^\alpha_{k\sigma} - E^\beta_{p+q\sigma} + \omega_q - \omega_{k-p}} + \frac{n^\beta_{k\sigma}(1 - n^\alpha_{p+q\sigma}) \sin^2\eta_{k\sigma} \cos^2\eta_{p+q\sigma}}{E^\beta_{k\sigma} - E^\alpha_{p+q\sigma} + \omega_q - \omega_{k-p}} \right]. \quad (22)$$

III. NUMERICAL RESULTS AND DISCUSSION

In this section we apply the general analytical results described above to the case of $Tl_2Mn_2O_7$, comparing the resulting spin excitations with the available experimental results.[22]

To evaluate the spin wave energies according to Eqs. (20)-(22), we need to perform sums over the first Brillouin zone (BZ) of the crystal lattice. Here we have adopted a simplification, assuming the lattice to be a simple cubic one, as already done previously,[15,18] since the effect of the detailed lattice structure is not central to the present discussion as we are studying ferromagnetic spin waves and considering a ferromagnetic superexchange interaction. This makes frustration effects due to the pyrochlore structure irrelevant.

With this simplification, the bare magnon energies are given by:

$$\omega_q = 2J_S M \left[(1 - \cos q_x a) + (1 - \cos q_y a) + (1 - \cos q_z a) \right], \quad (23)$$

where a is the lattice parameter.

To perform the BZ summations on the simple cubic lattice we have used the Chadi-Cohen process.[23,24] We noticed that to obtain dressed magnons with the appropriate symmetry of the lattice, it was not enough to use the basic wavevector set of the first BZ octant but that we needed to extend this set to the full first Brillouin zone, through the application of all the (48) symmetry operations of the O_h group.[25] We already found good convergence using the third order of the Chadi-Cohen BZ summation process.[23,24]

In Fig. 1 we show the bare isotropic ferromagnetic magnon energies along eight paths in the s.c. first BZ at temperature $T = 100K$, which would correspond to the results of the neutron scattering measurements.[22] Regarding the dressed magnon energies, evaluated as described in the previous section, the general trend is that the interaction of the local moments with the conduction electrons causes a softening of the ferromagnetic spin waves. The amplitude of the effect is however very small, consistently with the experimental data.[22] Of the two contributions to the renormalization, the longitudinal one (Eq. (22)) is almost negligible, being at least four orders of magnitude smaller than the bare energies. Therefore the renormalization seen in Fig. 1 is essentially due to the transverse contributions (Eq. (21)). It is worth mentioning that in Fig. 1 we are extending our perturbation calculation well beyond its expected range of convergence, because we choose $| J_H/J_S | > 1$ as was found appropriate for $Tl_2Mn_2O_7$.[18] This causes problems near $q = 0$, where the bare magnon energies are smaller than their negative renormalization contribution. Away from $q = 0$, we find a remarkable overall agreement in the whole BZ between the dressed ferromagnetic magnons which we obtain and the bare spin waves. This we ascribe to the fact that there are only few conduction electrons present in this compound,[1,3,15,18] as can be also seen in Fig. 2 depicting the band energies and indicating the Fermi level. There we see that the up-spin subbands for both α and β electrons are always higher in energy than their spin-down counterparts as expected from Eq. (8) since we have used $J_H < 0$. Also, the β states are almost empty while the down-spin α band is almost completely full.

It is interesting to mention that analyzing the effect of temperature on the dressed magnons calculated, we verified that we obtain the same trend which has been observed in the experiments,[22] namely, we do get a softening of the spin excitations as temperature increases though quantitatively our temperature effect is about one order of magnitude smaller than the measured one.

The following five figures have been included to allow a better understanding of the influence of the different parameters on the spin wave renormalization. We plot the results for a subset of non-equivalent wavevectors to allow visualization of the q-dependence of the renormalization.

Figs. 3 and 4 show the variation of the renormalized spin wave energy relative to its bare value versus, respectively, J_S and J_H, for a subset of seven non-equivalent wavevectors selected in the BZ. These two figures show opposite trends, which can be easily understood. As the magnitude of J_H grows with respect to that of J_S, the local moment system interacts more strongly with the itinerant electrons and the corresponding magnon energy acquires a larger renormalization. Conversely, if J_S grows with respect to J_H, the electronic effect on the magnons decreases, because the exchange energy now has the main role in determining the spin wave energy.

The following two figures show the effects of varying the electronic band parameters. While Fig. 5 shows that the renormalized magnon energy is rather insensitive to the hybridization t_{cd} (except for one of the wavevectors plotted), in Fig. 6 we observe that the bandwidth ratio t_d/t_c can have a sizeable effect, at least for wavectors away from the BZ boundaries. This effect might perhaps be explored experimentally in neutron scattering measurements under pressure.

In Fig. 7 we exhibit the effect of electron filling (even quite far above the ranges appropriate for the description of $Tl_2Mn_2O_7$[15,18]). As one would expect, the dressed magnon energies are quite sensitive to the electron filling, with quite larger magnitudes of spin wave softenings, monotonously increasing with n in the range showed.

Two common features are present in Figs. 3-7: one, that the renormalization generally results in a softening of the spin excitations by their coupling with the electrons; the other, that its magnitude is larger for wavevectors away from the Brillouin zone boundaries.

Our last figure (Fig. 8), was included to exhibit the effect of a change of sign of the Hund coupling J_H on the renormalized magnons, in this case favouring FM alignment of the d-electron spins with the local spins (it is worth mentioning that the ground state of the generic model is symmetric with respect to such sign change if accompanied by a reversal of the relative spin orientations of the local moments and $d-$spins, as discussed in Ref. 18). Such sign change reverses the relative order of the spin up and down electron eigenbands: the longitudinal magnon renormalization contribution (Eq. (22)) therefore changes sign; the transversal contribution (see Eq. (21)), dominating the magnon renormalization as mentioned above, changes in a less obvious way under sign reversal of the Hund coupling, leading to the dressed magnons depicted in Fig. 8. Here a hardening of the magnons away from the long wavelenghts' region is visible, contrary to the softening observed on the whole BZ when the Hund coupling favours antiparallel alignment of the d-electron spins with respect to the local spins. This is an interesting prediction, being the discussion of the sign of such Hund coupling in $Tl_2Mn_2O_7$ a non-settled matter (e.g. in Refs. 21 and 6 an antiparallel alignment due to the Hund coupling is mentioned, while e.g. in Refs. 16 and 26 the opposite case is proposed), as it would provide a tool to determine experimentally such sign by measuring the magnons with neutron scattering experiments on $Tl_2Mn_2O_7$ performed in the yet unexplored shorter wavelenghts' region of the BZ.

IV. SUMMARY

In the present work, we have addressed the problem of the spin excitations measured in $Tl_2Mn_2O_7$,[22] found to exhibit features characteristic of isotropic ferromagnets and contrasting starkly with the results in CMR perovskites. Using the generic model[18] to describe the compound, assuming a ferromagnetic superexchange interaction between the Mn^{4+} spins, we have employed a perturbative approach to calculate the magnon dispersion relation along different paths in the first Brillouin zone. In such way, we were able to describe qualitatively the available experimental results, using parameters for the generic model as found appropriate for the description of $Tl_2Mn_2O_7$ before.[18]

Even though in the present work we are extending our perturbative calculation well beyond its expected range of convergence by the magnetic coupling parameters used (resulting in problems near $q = 0$: where bare magnon energies are smaller than their renormalization), a remarkable overall agreement along the Brillouin zone is evident between the dressed ferromagnetic magnons obtained from the generic model and the bare spin waves (characteristic of an ideal isotropic ferromagnet, such as found in experiments.[22]) This is due to the electronic structure particularities and the small number of effective carriers in $Tl_2Mn_2O_7$.[3,15,6,18] A measurement of the magnon dispersion relations at smaller wavelenghts, should allow to distinguish if the Hund coupling favours parallel or antiparallel alignment of the Mn^{4+} spins and the narrow band electrons, according to the present predictions of a hardening or softening, respectively, of the dressed magnons in such cases. According to our results, there should also be a sizeable effect of pressure upon the spin excitations, corresponding to the ensuing variation of the relative electron bandwidths of the generic model, which it would also be interesting to study experimentally.

ACKNOWLEDGMENTS

C.I.V. thanks Jeff Lynn for drawing her attention to this problem and for enlightening discussions. Both authors thank B.Alascio for his interest and comments. C.I.V. is a member of the Carrera del Investigador Científico of CONICET (Consejo Nacional de Investigaciones Científicas y Técnicas, Argentina), and wishes to acknowledge the financial support and hospitality of the Dipartimento di Fisica, Universitá di Parma, and International Centre for Theoretical Physics, Trieste, where part of this work was done. M.A. acknowledges financial support of I.N.F.M. and the hospitality of Centro Atómico Bariloche.

---

[1] Y. Shimakawa, Y. Kubo, and T. Manako, Nature 379, 55(1996); Y. Shimakawa, Y. Kubo, T. Manako, Y. V. Sushko, D. N. Argyriou, and J. D. Jorgensen, Phys. Rev. B **55**, 6399 (1997).
[2] S. W.Cheong, H. Y. Hwang, B. Batlogg, and L. W. Rupp Jr., Solid State Commun. **98**, 163 (1996).
[3] M. A. Subramanian, B. H. Toby, A. P. Ramirez, W. J. Marshall, A. W. Sleight, and G. H. Kwei, Science **273**, 81 (1996).
[4] R. von Helmolt, J. Wecker, B. Holzapfel, L. Schultz, and K. Samwer, Phys. Rev. Lett. **71**, 2331 (1993); S. Jin, T. H. Tiefel, M. McCormack, R. A. Fastnacht, R. Ramesh, and L. H. Chen, Science **264**, 413 (1994).
[5] G. H. Kwei, C. H. Booth, F. Bridges, and M. A. Subramanian, Phys. Rev. B **55**, R688 (1997).
[6] H. Imai, Y. Shimakawa, Y. V. Sushko, and Y. Kubo, Phys. Rev. B **62**, 12190 (2000).
[7] Y. V. Sushko, Y. Kubo, Y. Shimakawa, and T. Manako, Czech. J. Phys. **46**, 2003 (1996); Y. V. Sushko, Y. Kubo, Y. Shimakawa, and T. Manako, Rev. High Pressure Sci. Tech. **7**, 505 (1998); Y. V. Sushko, Y. Kubo, Y. Shimakawa, and T. Manako, Physica B **259-261**, 831 (1999).
[8] M. Núñez Regueiro *et al.*, in *Proceedings of the MRS Meeting, Boston, 1999.*
[9] T. Takeda *et al.*, J. Sol. State Chem. **140**, 182 (1998); B. Martínez *et al.*, Phys. Rev. Lett. **83**, 2022 (1999); R. Senis *et al.*, Phys. Rev. B **61**, 11637 (2000).
[10] A. P. Ramirez and M. A. Subramanian, Science **277**, 546 (1997).
[11] J. A. Alonso *et al.*, Phys. Rev. B **60**, 15024 (1999).
[12] J. A. Alonso, J. L. Martínez, M. J. Martínez-Lope, M. T. Casais, and M. T. Fernández-Díaz, Phys. Rev. Lett. **82**, 189 (1999).
[13] J. A. Alonso, M. J. Martínez-Lope, M. T. Casais, J. L. Martínez, and M. T. Fernández-Díaz, Chemistry of Materials **12**, 1127 (2000).
[14] J. A. Alonso *et al.*, Appl. Phys. Lett. **76**, 3274 (2000); P. Velasco, J. A. Alonso, M. T. Casais, M. J. Martínez-Lope, J. L. Martínez, and M. T. Fernández-Díaz, Phys. Rev. B **66**, 174408 (2002).
[15] C. I. Ventura and B. Alascio, Phys. Rev. B **56**, 14533 (1997); C. I. Ventura and B. Alascio, in *Current Problems in Condensed Matter*, edited by J. L. Morán-López (Plenum Press, New York, 1998), p. 27.
[16] P. Majumdar and P. B. Littlewood, Phys. Rev. Lett. **81**, 1314 (1998).
[17] M. D. Núñez-Regueiro and C. Lacroix, Phys. Rev. B **63**, 14417 (2001).
[18] C.I.Ventura and M.A.Gusmão, Phys. Rev. B **65**, 14422 (2002).
[19] D. K. Seo, M. H. Whangbo, and M. A. Subramanian, Solid State Commun. **101**, 417 (1997).
[20] D. J. Singh, Phys. Rev. B **55**, 313 (1997).
[21] S. K. Mishra and S. Satpathy, Phys. Rev. B **58**, 7585 (1998).
[22] J.W.Lynn, L.Vasiliu-Doloc and M.A. Subramanian, Phys. Rev. Lett. **80**,4582(1998).
[23] D.J. Chadi and M.L.Cohen, Phys. Rev. B **8**, 5747 (1973).
[24] L.Macot and B.Frank, Phys. Rev. B **41**, 4469 (1990).
[25] M.Tinkham, "Group Theory and Quantum Mechanics", McGraw-Hill Book Co., New York (1964).
[26] P. Velasco *et al.*, Phys. Rev. B **66**, 104412 (2002).

Fig. 1. Spin wave dispersion relations along eight trajectories in the s.c. first Brillouin zone: bare ferromagnetic magnons (solid line) vs. dressed magnons calculated (points). Energies in units of t_c; origin: $\epsilon_c = 0$. Other parameters of the generic model for $Tl_2Mn_2O_7$: $\epsilon_d = -0.7$; $t_d = 0.1$; $t_{cd} = 0.3$; $n = 1.07$; $J_S = 0.2$; $J_H = -0.9$. BZ points: $0 = \Gamma = (0,0,0)$, $X = (\pi/a, 0, 0)$, $Y = (0, \pi/a, 0)$, $Z = (0, 0, \pi/a)$, $M = (\pi/a, \pi/a, 0)$ and $L = (\pi/a, \pi/a, \pi/a)$.

Fig. 2. Bare electronic spin subband dispersion relations, along eight trajectories in the s.c. first Brillouin zone: $E_{\alpha\uparrow}$ (solid); $E_{\alpha\downarrow}$ (long dashes); $E_{\beta\uparrow}$ (short dashes); $E_{\beta\downarrow}$ (dotted). Fermi level: $\mu/t_c = -1.47$. BZ points and parameters as in Fig. 1.

Fig. 3. Magnon renormalization factor ($= \tilde{\omega}_q/\omega_q$) vs. superexchange coupling, J_S, for seven non-equivalent wave-vectors (indicated as $q_1 - q_7$ along the abcissa of Fig. 1). $J_H = -0.8$; other parameters as in Fig. 1.

Fig. 4. $\tilde{\omega}_q/\omega_q$ vs. magnitude of the Hund coupling, $\mid J_H \mid$, for the same non-equivalent wave-vectors of Fig. 3. $J_S = 0.1$; other parameters as in Fig. 1.

Fig. 5. $\tilde{\omega}_q/\omega_q$ vs. hybridization, t_{cd}, for the same non-equivalent wave-vectors of Fig. 3. $J_S = 0.1; J_H = -0.8$; other parameters as in Fig. 1.

Fig. 6. $\tilde{\omega}_q/\omega_q$ vs. relative bandwidth, t_d/t_c, for the same non-equivalent wave-vectors of Fig. 3. Other parameters as in Fig. 5.

Fig. 7. $\tilde{\omega}_q/\omega_q$ vs. total electron filling, n, for the same non-equivalent wave-vectors of Fig. 3. Other parameters as in Fig. 5.

Fig. 8. Spin wave dispersion relations along eight trajectories in the s.c. first BZ: bare ferromagnetic magnons (solid line) vs. dressed magnons calculated (points). $J_H = +0.8$; $J_S = 0.4$; other parameters as in Fig. 1.

Fig. 1 - C. I. Ventura - PRB

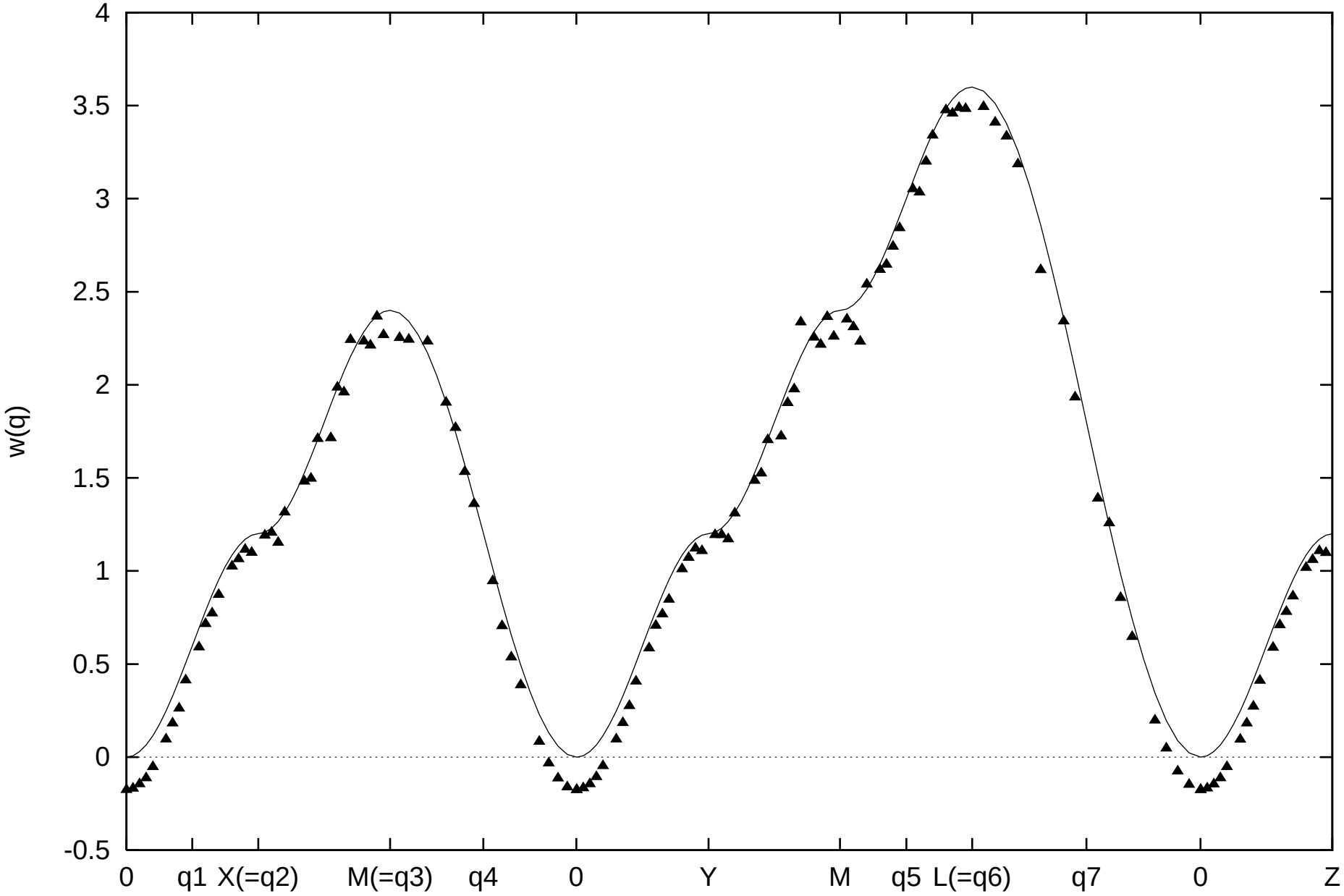

Fig. 2 - C. I. Ventura - PRB

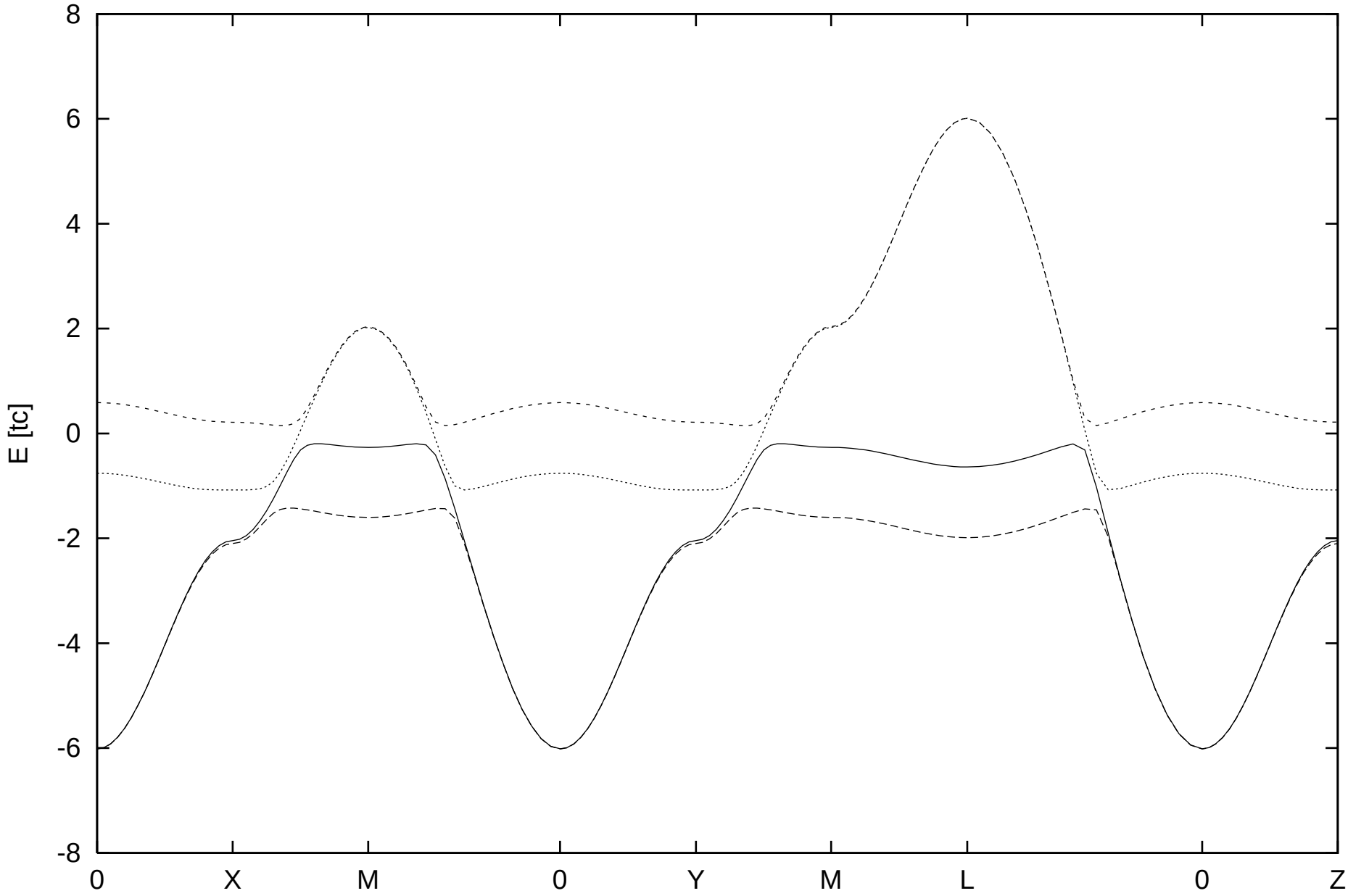

Fig. 3 - C. I. Ventura - PRB

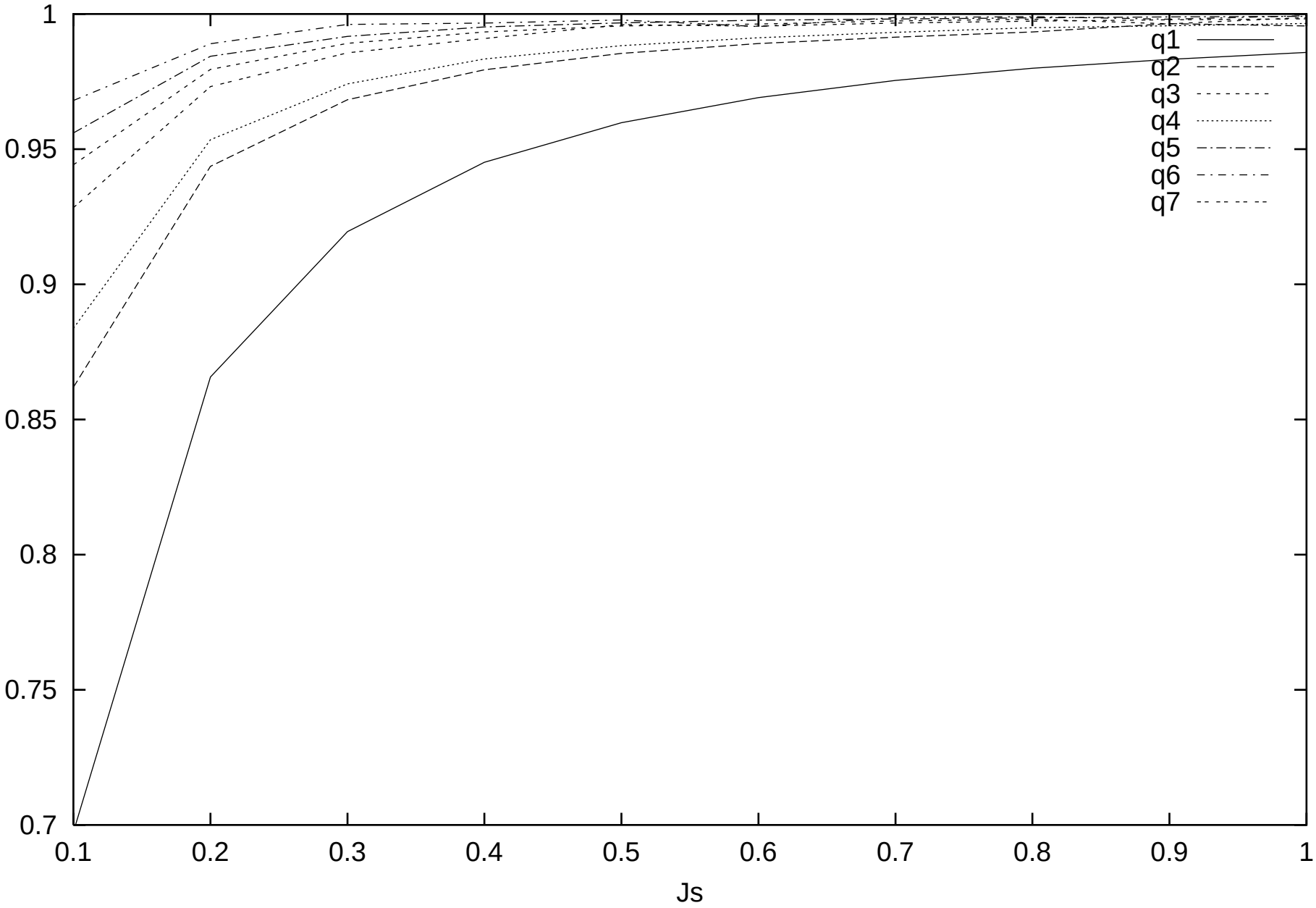

Fig. 4 - C. I. Ventura - PRB

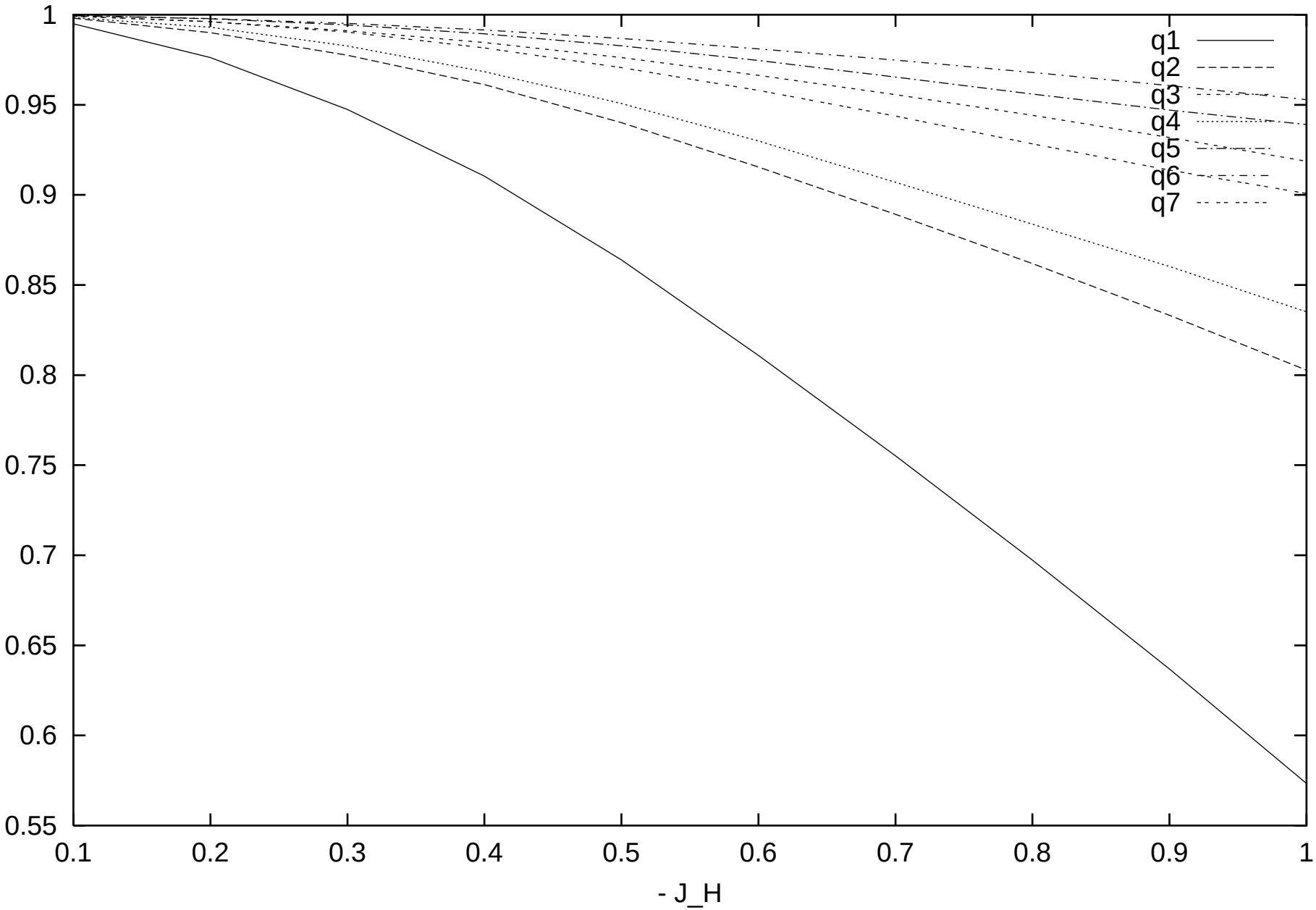

Fig. 5 - C. I. Ventura - PRB

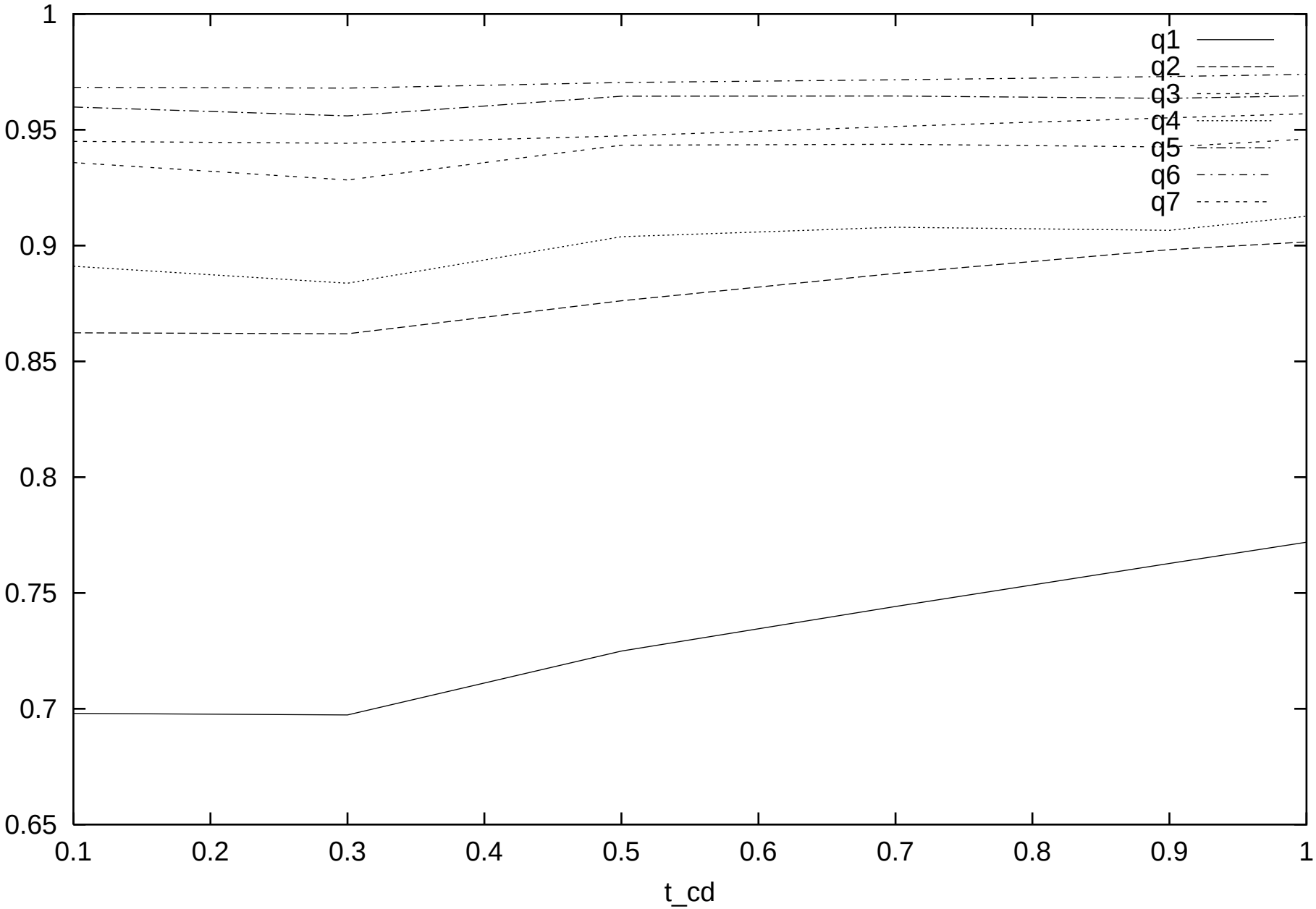

Fig. 6 - C. I. Ventura - PRB

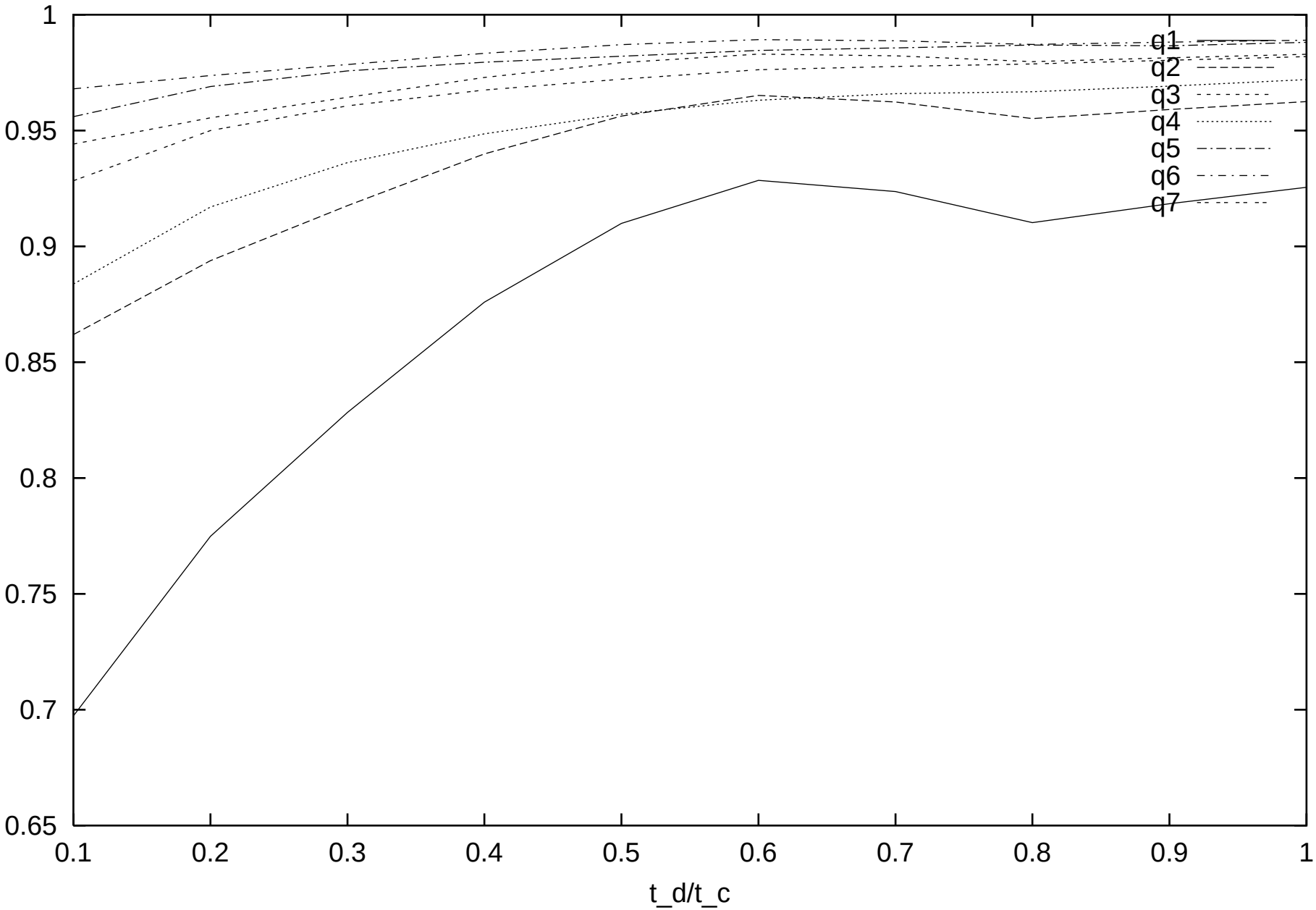

Fig. 7 - C. I. Ventura - PRB

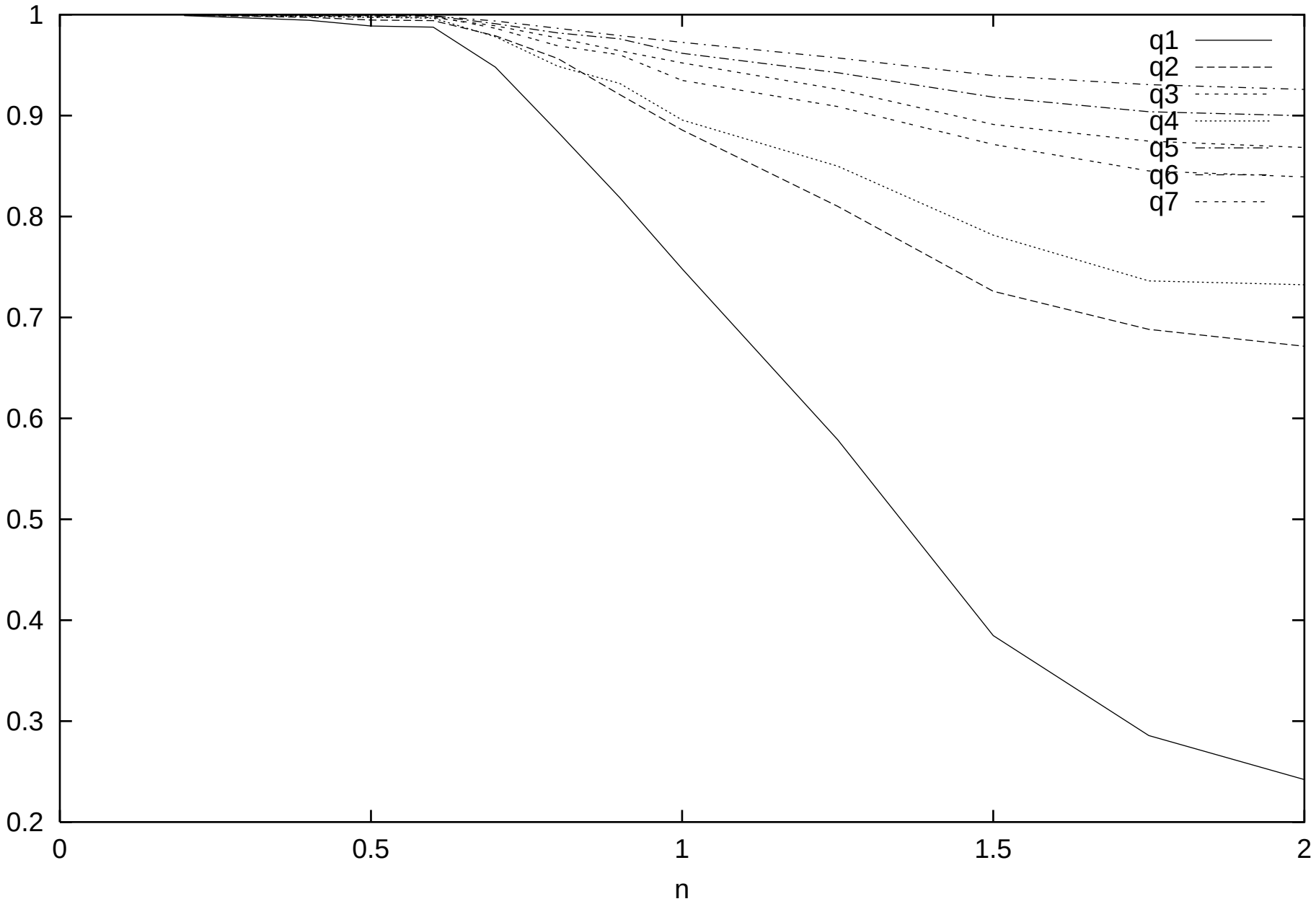

Fig. 8 - C. I. Ventura - PRB